Journal of Zhejiang University-SCIENCE A (Applied Physics & Engineering)
ISSN 1673-565X (Print); ISSN 1862-1775 (Online)
www.jzus.zju.edu.cn; link.springer.com
E-mail: jzus_a@zju.edu.cn

Catalytic effects of V_2O_5 on oxidative pyrolysis of spent cation exchange resin[#*]

Qi SONG[1,2], Jian-hua SHEN[1,2], Yong YANG[1,2], Yao YANG[†‡1,2], Bin-bo JIANG[1,2], Zu-wei LIAO[1,2,3]

[1]*Zhejiang Provincial Key Laboratory of Advanced Chemical Engineering Manufacture Technology, Zhejiang University, Hangzhou 310027, China*

[2]*College of Chemical and Biological Engineering, Zhejiang University, Hangzhou 310027, China*

[3]*State Key Laboratory of Chemical Engineering, College of Chemical and Biological Engineering, Zhejiang University, Hangzhou 310027, China*

[†]E-mail: yao_yang@zju.edu.cn

Received Mar. 16, 2020; Revision accepted Sept. 4, 2020; Crosschecked Jan. 12, 2021

Abstract: Pyrolysis is a cost-effective and safe method for the disposal of radioactive spent resins. In this work, the catalytic effects of V_2O_5 on the pyrolysis of cation exchange resin are investigated for the first time. The results show that it is a better catalyst than others so far studied and achieves a lowering of final pyrolysis temperature and residual rate simultaneously when aided by physical blending. The maximum reductions of the final pyrolysis temperature and the residual rate are 173 °C and 11.9% (in weight), respectively. Under the action of V_2O_5, low-temperature (445 °C) removal of partial sulfonic acid groups occurs and the pyrolysis of the resin copolymer matrix is promoted. This is demonstrated by the analysis of pyrolysis residues at different temperatures by X-ray photoelectron spectroscopy (XPS) and element analysis. The catalytic activity of V_2O_5 is determined by effects both at acid sites and oxidation-reduction centers via H_2-TPR (temperature programmed reduction), O_2-TPD (temperature programmed desorption), CO_2-TPD, and NH_3-TPD. The catalytic effect of oxidation-reduction centers in V_2O_5 is achieved by close contact with the sulfur bond through chemisorption under the effect of acid sites. V_2O_5 is also believed to be the reason for the removal of partial sulfonic acid groups at lower temperatures (445 °C). V_2O_5 is an effective catalyst for spent resin pyrolysis and can be further applied in industry.

Key words: Waste disposal; Cation exchange resin; V_2O_5; Catalysis; Oxidative pyrolysis
https://doi.org/10.1631/jzus.A2000100 **CLC number:** O643.3

1 Introduction

Nuclear power plants produce a large amount of radioactive spent ion exchange resins containing ^{60}Co, ^{137}Cs, ^{90}Sr, and ^{14}C (Wang and Wan, 2015). The radioactivity from these spent resins is about 80% of the total activity of low- and intermediate-level radioactive wastes (Zhang and Li, 2015). Therefore, much attention has been paid to the safe disposal and minimization of these radioactive spent resins. At present, the treatment methods (Jantzen et al., 2013; Wang and Wan, 2015; Zhang and Li, 2015) for them include cementation, bituminization, plastic solidification, glass solidification (Hamodi et al., 2012), super compaction, incineration, supercritical water oxidation (Kim et al., 2010), plasma oxidation (Nezu et al., 2003; Moustakas et al., 2005), Fenton oxidation (Zahorodna et al., 2007; Wan et al., 2016), molten salt oxidation (Eun et al., 2009; Yang et al., 2013), and steam reforming technology (Jantzen, 2006; Jantzen

‡ Corresponding author
* Project supported by the National Natural Science Foundation of China (No. U1862203), the National Science Fund for Distinguished Young Scholars (No. 21525627), and the Science Fund for Creative Research Groups of National Natural Science Foundation of China (No. 61621002)
# Electronic supplementary materials: The online version of this article (https://doi.org/10.1631/jzus.A2000100) contains supplementary materials, which are available to authorized users
ORCID: Yao YANG, https://orcid.org/0000-0003-3611-2859

et al., 2007; Mason and Myers, 2010; Pierce et al., 2014; Song et al., 2020). It is worth noting that although incineration can greatly reduce the volume of waste, it leads to the volatilization of radionuclides at high temperatures (Yang et al., 2013), so it is not suitable for the disposal of radioactive spent resins. By steam reforming technology, spent resins are converted into CO_2 and H_2O by oxidative pyrolysis, and the nuclides are immobilized by minerals. This method has the advantages of a high volume reduction ratio, no pollution of the exhaust gas, and good stability of the residue (Jantzen, 2006; Jantzen et al., 2007; Mason and Myers, 2010). The pyrolysis process can be divided into three stages (Matsuda et al., 1986a; Juang and Lee, 2002): first, dehydration; second, decomposition and transformation of sulfonic acid groups; finally, the decomposition of the copolymer matrix. In the second stage, the sulfonic acid group transforms into the sulfur bond (-S-), which forms a cross-linked structure with the copolymer matrix and inhibits the pyrolysis reaction (Matsuda et al., 1987; Chun et al., 1998). Apparently, this is contrary to the requirement for a high volume-reduction ratio. Moreover, to destroy the cross-linked polymer structures, the reaction temperature needed is very high, which may cause the volatilization of radionuclides, such as Cs. Therefore, developing methods to decrease the residual rate, which is defined as the percentage of the residue obtained after pyrolysis, and simultaneously also decrease the pyrolysis temperature, has become a problem of concern.

Previous investigation has proved that catalytic pyrolysis is a feasible method for decreasing the pyrolysis temperature of cation exchange resins (Singare et al., 2011). Matsuda et al. (1986b) found that doped metal ions, such as Pd^{2+}, Cu^{2+}, Fe^{2+}, Fe^{3+}, and Co^{2+} (at a concentration of 0.5 mmol/L dry resin), increased the reaction rate constant of the oxidative pyrolysis of cation exchange resins. It was explained that these metal ions could combine with sulfur in the sulfonic acid group to form sulfides, which were subsequently oxidized to oxides under the action of oxygen. These metal oxides may have a catalytic effect on the pyrolysis reaction of resins. Juang and Lee (2002) found that some metal salts and metal oxides, such as $CuSO_4{\cdot}5H_2O$ and CuO, also had a catalytic effect on the oxidative pyrolysis of cation exchange resins. The final pyrolysis temperature decreased with increase in the additive. The catalytic effect of metal salts was also explained as the catalytic effect of metal oxides. During the reaction, $CuSO_4{\cdot}5H_2O$ and CuO would transform into Cu_2O, with many oxygen vacancies in the crystal lattice. These oxygen vacancies were excellent adsorption sites for oxygen, and the absorbed reactive oxygen species enhanced the oxidative pyrolysis of the organic copolymer matrix (Freund et al., 1996; Triguero et al., 1999; Juang and Lee, 2002; Wang and Barteau, 2003). Superficially, Juang and Lee (2002) agreed well with Matsuda et al. (1986b). Whether the additive was doped metal ions, metal salts or metal oxides, the catalytic effect was attributed to the oxidability of metal oxides. However, Matsuda et al. (1986a) found that when directly adding Fe_2O_3 and Fe_3O_4, there was little catalytic effect on the oxidative pyrolysis of resins compared with doped Fe^{2+} and Fe^{3+}. This was explained by assuming that doped Fe^{2+} and Fe^{3+} would be uniformly distributed inside the resin particles and thus have a large contact area, while the non-ionic Fe_2O_3 and Fe_3O_4 were distributed only on the surface of the particles. This is in apparent contradiction with the mechanism of the catalytic effect of CuO on cation exchange resins proposed by Juang and Lee (2002). Therefore, the mechanism of the above catalysts on the pyrolysis of cation exchange resin is unclear, and some unexplained experimental phenomena remain.

On the other hand, in previous research, the pyrolysis temperature of resins was shown to be lowered by adding a catalyst, but there was no obvious change in the amount of pyrolysis residue of the resin. Although it has been known that the sulfur bond (-S-) formed during the reaction inhibits the oxidative pyrolysis of the copolymer matrix, there are few reports on the decomposition of sulfur bonds in resins in the literature. Myrstad et al. (2000) found that vanadium-based catalysts had an obvious desulfurization capacity, which could effectively reduce the sulfur content in fluid catalytic cracking (FCC) gasoline, in which thiophene sulfides account for 95% and have similar sulfur bond structure (-S-). Thus, in view of the significant desulfurization ability of vanadium compounds (Myrstad et al., 2000; Sviridova et al., 2013; Tomskii et al., 2017), the catalytic effect of V_2O_5 on oxidative pyrolysis of cation exchange resin

is investigated in this work. It was expected to decrease the resin residual rate while decreasing the pyrolysis temperature.

The whole work is organized as follows. Firstly, V_2O_5 is added by physical blending to investigate its catalytic effect on the pyrolysis of resins in the thermogravimetric analyzer and tube furnace. Secondly, the catalytic effect of V_2O_5 is compared with other typical catalysts through X-ray photoelectron spectroscopy (XPS) and elemental analysis of the pyrolysis residue. Finally, combined with the analyses of H_2-temperature programmed reduction (TPR), O_2-temperature programmed desorption (TPD), CO_2-TPD, and NH_3-TPD of various catalysts, the catalytic mechanism is further revealed.

2 Experimental

2.1 Experimental materials

The main material used in this study is Amberlite IRN-97H cation exchange resin supplied by the Rohm & Haas Company, USA. The resin consists of sulfonic acid groups (-SO_3H) and an insoluble skeleton formed by copolymerization of styrene and divinylbenzene. In addition, the catalysts used for pyrolysis of resins include V_2O_5 (99.99%, Shanghai Macklin Biochemical Co., Ltd., China), CoO (analytical reagent (AR), Aladdin Reagent Co., Ltd., China), Co_2O_3 (AR, Shanghai Macklin Biochemical Co., Ltd., China), Co_3O_4 (AR, Shanghai Macklin Biochemical Co., Ltd., China), and CuO (99%, Shanghai Macklin Biochemical Co., Ltd., China).

2.2 Experimental methods

Thermogravimetric experiments on resins were performed on the TGA/DSC 3+ thermogravimetric analyzer from the Mettler Toledo Company, Switzerland. Resins were first dried and ground into powders (average diameter of 85 μm), and then mixed with catalyst powders at different catalyst/resin mass ratios of 0.05, 0.10, 0.15, and 0.20 by physical blending. The mixture was heated from 30 °C to 900 °C at a heating rate of 10 °C/min in an air flow of 60 mL/min.

Pyrolysis experiments under different temperatures were conducted in a TL1200-S-II tube furnace (Nanjing Boyuntong Co., Ltd., China). The resin powders and catalyst powders at the catalyst/resin mass ratio of 0.10 were first mixed and transferred to the crucible. Then the mixture was put into the tube furnace and reacted at different temperatures (350 °C, 445 °C, 515 °C, 630 °C, and 760 °C) for 30 min in an air flow of 300 mL/min.

2.3 Calculation and analysis method

Considering the effects of water content of resins and the amount of catalyst added in the mass fraction of residue, the percentage of residue obtained after pyrolysis (residual rate) is calculated as follows:

1. If the initial mass of resin is m_0, and the catalyst/resin mass ratio is α, then the amount of catalyst added is $m_0\alpha$.

2. If the weight loss rate of resin in the water removal stage is measured as w_w (generally about 7%–10%), then the mass of the reactant after removal of water is $m_0(1+\alpha)(1-w_w)$.

3. If the residual ratio of the reactant is w_R, then the mass of residue is $m_0(1+\alpha)(1-w_w)w_R$, which contains residual catalyst and resin pyrolysis product.

4. According to the thermogravimetric curves of each catalyst as shown in Fig. S1, there is no obvious weight loss below 800 °C, and thus the mass of the catalyst in the residue is still $m_0\alpha$. Then the mass of the resin pyrolysis product is $m_0[(1+\alpha)(1-w_w)w_R-\alpha]$, and the residual rate is $m_0[(1+\alpha)(1-w_w)w_R-\alpha]/[m_0(1+\alpha)(1-w_w)-m_0\alpha]$, which can be simplified to $w_R-\alpha/[(1+\alpha)(1-w_w)]$.

XPS analysis of the solid residue was performed on the ESCALAB 250Xi X-ray photoelectron spectrometer (Thermo Fisher Scientific, USA). The element analysis of the solid residue was performed on the Vario EL III elemental analyzer (Elementar Analysensysteme GmbH, Germany). The H_2-TPR, O_2-TPD, CO_2-TPD, and NH_3-TPD analyses of catalysts were performed on the Autosorb IQ-C-TCD physicochemical adsorption instrument (Quantachrome Instruments, USA).

3 Results and discussion

3.1 Oxidative pyrolysis of resin under the catalytic effects of V_2O_5

The thermogravimetric curves of the resins with different added amounts of V_2O_5 are shown in Fig. 1.

The addition of V_2O_5 mainly affects the weight loss behavior at the fourth weight loss peak (Peak 4), which is related to the destruction of the copolymer matrix (Juang and Lee, 2002; Eun et al., 2009). The characteristic values in the curves are presented in Table 1. As shown in Fig. 1b, the first and second weight loss peaks of pure resin appear at 280–400 °C and 400–480 °C, respectively. According to the literature (Matsuda et al., 1987; Chun et al., 1998), there is partial-SO_3H transformation into SO_2 and the others form the sulfone group (-SO_2-) and sulfur bond (-S-) under these temperatures. The escape of SO_2 causes the weight loss. Since the sulfur bond is embedded in the copolymer matrix to form a stable structure, there is no obvious weight loss for pure resin at 500–710 °C. As the temperature increases further, the copolymer matrix is pyrolyzed and the weight loss peak occurs at 710–830 °C.

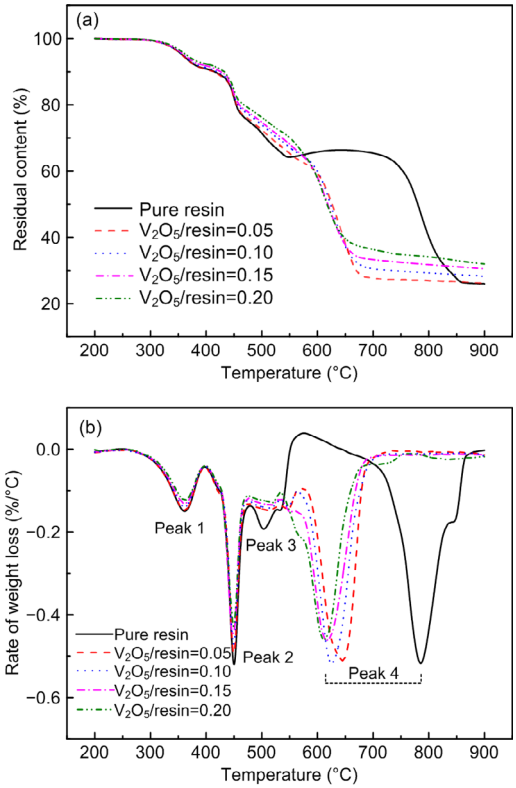

Fig. 1 Thermogravimetric curves of the resin with different amounts of V_2O_5: (a) thermogravimetric (TG) curves; (b) derivative thermogravimetric (DTG) curves

The pyrolysis temperature and weight loss rate of the resin mixed with different amounts of V_2O_5 are basically the same as those of pure resin at the first peak (280–400 °C) and the second peak (400–480 °C), which indicates that V_2O_5 has little effect on the removal and conversion of sulfonic acid groups. At the third peak (480–570 °C), the initial temperature of the weight loss peak is basically unchanged after adding V_2O_5, but the terminal temperature of the weight loss peak and the weight loss rate both increase. This may be due to V_2O_5 promoting the decomposition of -SO_2-. At the fourth one (about 560–830 °C), with the increase in the added amount of V_2O_5, the initial temperature, terminal temperature, and peak temperature of the weight loss peak and the mass fraction of the pyrolysis product all decrease. When the mass ratio of V_2O_5 to resin is 0.05 to 0.20, the peak temperature of the weight loss peak is lowered by 140 °C to 173 °C, and the mass fraction of the pyrolysis product is decreased by 5% to 11.9%. The results show that V_2O_5 can decrease the residual rate of the resin while reducing the pyrolysis temperature.

3.2 Performance comparison between V_2O_5 and other catalysts

To further explore the catalytic effect of V_2O_5 on the oxidative pyrolysis of resin, the relative catalytic performance of V_2O_5 and other catalysts was compared. As described in the Introduction, there are mainly three types of catalysts used for this reaction: metal ions (such as Pd^{2+}, Cu^{2+}, Fe^{2+}, Fe^{3+}, and Co^{2+}), metal sulfates (such as $CuSO_4{\cdot}5H_2O$), and metal oxides (such as CuO). It is believed that metal sulfates form metal oxides during the oxidative pyrolysis reaction and these oxides act as catalysts. Therefore, doped Co^{2+} and different metal oxides were selected as comparative catalysts in this work. The metal

Table 1 Comparison of pyrolysis behaviors of resins with different amounts of V_2O_5

Mass ratio of V_2O_5 to resin	Initial temperature of Peak 4 (°C)	Terminal temperature of Peak 4 (°C)	Peak temperature of Peak 4 (°C)	Weight loss rate of Peak 4 (%)	Residual rate (%)
0	710	830	785	37.9	25.9
0.05	573	700	645	34.6	20.9
0.10	566	690	625	35.2	18.2
0.15	564	680	616	33.5	16.2
0.20	560	676	612	33.8	14.0

oxides contain CuO, Co_2O_3, Co_3O_4, and CoO, and the amount added is 5% of the resin. If Co^{2+} is doped on the resin with a catalyst/resin weight ratio of 5% like other metal oxides, the doped concentration is 75 g/L, which exceeds the exchange capacity of the cation exchange resin. In addition, in the previous study (Shen et al., 2019), it is found that when the doped Co^{2+} is more than 10 g/L, the catalytic effect is basically unchanged. Thus, the results with a doped amount of 10 g/L were chosen for comparison.

Compared to the oxidative pyrolysis of pure resin, the changes of final pyrolysis temperature and residual rate under the influence of different catalysts are shown in Fig. 2. CuO and various oxides of Co have almost no catalytic effect under the same conditions, while doped Co^{2+} decreases the final pyrolysis temperature significantly. This is consistent with the results of Matsuda et al. (1986a, 1986b), who found that doped Fe^{2+} had a catalytic effect on the oxidative pyrolysis of resin while directly adding Fe_2O_3 or Fe_3O_4 did not. According to previous studies (Matsuda et al., 1986b; Shen et al., 2019), the doped Co^{2+} is combined with the sulfonic acid group through a chemical bond, and the cobaltous oxide formed is well dispersed in the resin during the pyrolysis process. The uniformly distributed cobaltous oxide will be in full contact with sulfur groups to supply reactive oxygen. For the physical blending of CuO or various oxides of Co, the contact efficiency between catalysts and sulfur groups is so low that a catalytic effect is not evident. However, comparing the catalytic performance of V_2O_5 with that of other metal oxides, it can be found that although V_2O_5 is also added by physical blending, it decreases the final pyrolysis temperature significantly. Moreover, although the decrease of final pyrolysis temperature is not as large as that of doped Co^{2+}, V_2O_5 is the only catalyst under which the residual rate of resin is significantly decreased. In addition, the reduction of final pyrolysis temperature and residual rate under the catalytic effect of V_2O_5 are clearly higher than the results in the literature (Juang and Lee, 2002).

In order to further compare the catalytic effect of Co^{2+} and V_2O_5, the pure resin, Co^{2+}-doped resin, and V_2O_5-mixed resin (the mass ratio of V_2O_5 to resin is 0.10) are pyrolyzed at different temperatures, and the solid residues are analyzed by XPS and the results are shown in Fig. 3. As shown in Fig. 3, S 2p exhibits four peaks in XPS spectrums of residue, located at 169.1 eV, 168.9 eV, 168.2 eV, and 163.8 eV, representing the sulfonic acid group ($-SO_3H$), sulfate sulfur (SO_4^{2-}), sulfone sulfur ($-SO_2-$), and organic sulfur bond (-S-), respectively (Hu et al., 2014; Hou et al., 2018; Tang et al., 2018). For the pure resin shown in Fig. 3a, the $-SO_3H$ in the raw resin is first converted to $-SO_2-$ at 350 °C, then partial $-SO_2-$ transforms into -S-

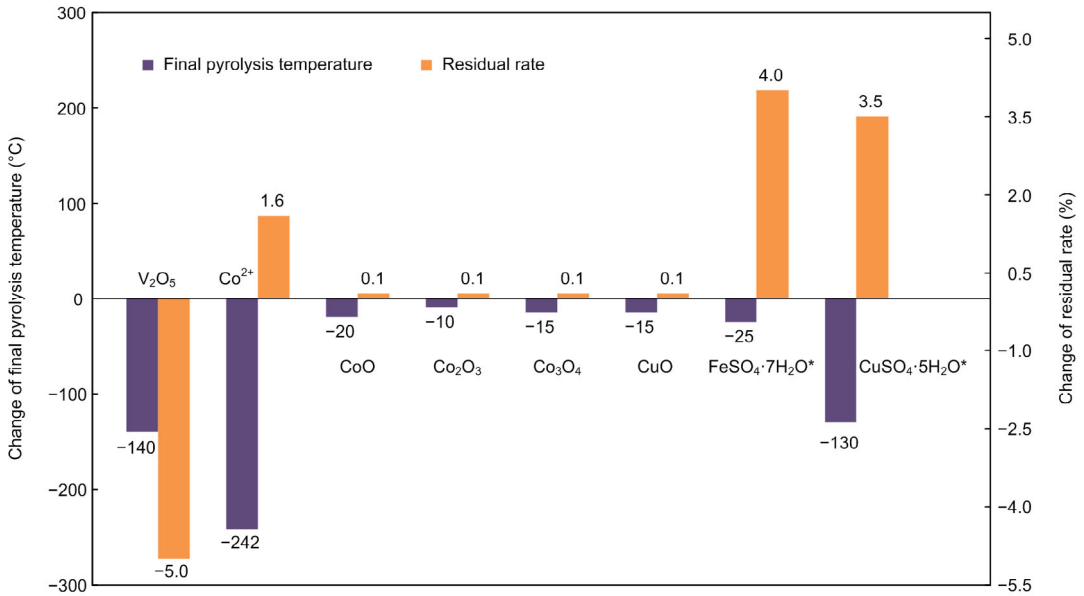

Fig. 2 Performance comparison of different catalysts for oxidative pyrolysis of resin

* Results from Juang and Lee (2002)

at 445 °C. At 515 °C and 630 °C, the sulfur is mainly present in the forms of SO_4^{2-} and -S-. Finally, -S- completely decomposes and the form of sulfur in the pyrolysis residue is mainly SO_4^{2-} at 760 °C. For the Co^{2+}-doped resin (Fig. 3b), the -S- is already formed in the residue at 350 °C and decomposes and transforms into SO_4^{2-} at 515 °C. This shows that the doped Co^{2+} can promote the conversion and decomposition of -S- at lower temperatures (350–445 °C), that is why doped Co^{2+} decreases the final pyrolysis temperature. For the V_2O_5-mixed resin (Fig. 3c), the $-SO_3H$ transforms into $-SO_2-$ at 350 °C, which is consistent with the pure resin. Then partial $-SO_2-$ is converted to SO_4^{2-}, and the other part transforms into -S- at 445 °C. Finally, the formed -S- is completely decomposed at 630 °C. V_2O_5 can promote the formation of SO_4^{2-} at a lower temperature (445 °C) and decrease the decomposition temperature of -S-.

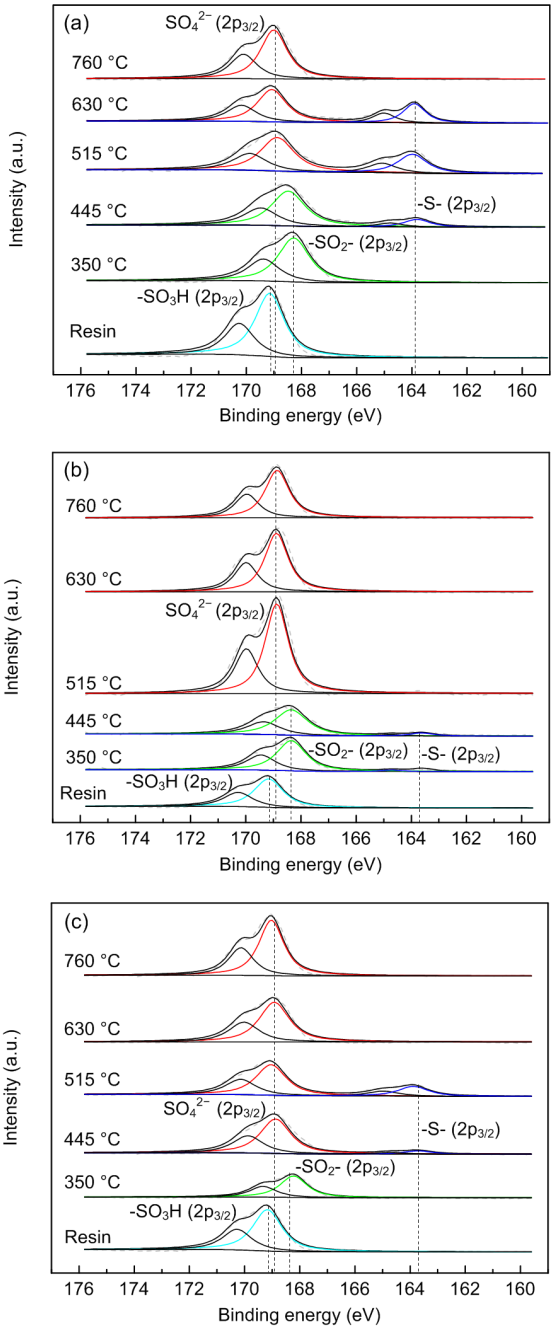

Fig. 3 XPS spectrums of pyrolysis residue at different temperatures: (a) pure resin; (b) Co^{2+}-doped resin; (c) V_2O_5-mixed resin

With a view to quantitatively characterizing the change of the $-SO_3H$ and the copolymer matrix during the resin pyrolysis process, the solid residues were subjected to elemental analysis and the results are presented in Fig. 4. Combining with Fig. 3, for pure resins, most of C decreases when the temperature increases from 515 °C to 630 °C, which indicates that since -S- is formed, the copolymer matrix can only be decomposed at higher temperatures. However, the C content of Co^{2+}-doped resin is significantly decreased

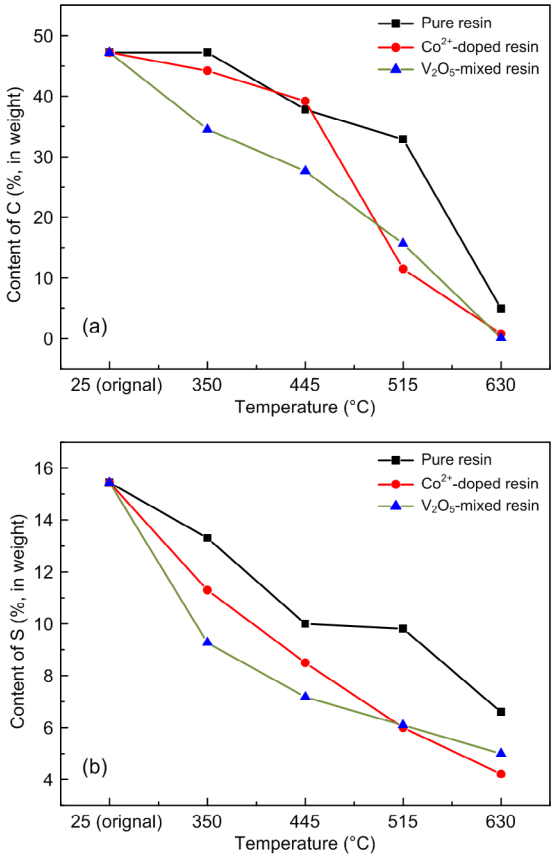

Fig. 4 Elemental analysis of pyrolysis residue at different temperatures: (a) content of C; (b) content of S

at 515 °C, indicating that the decomposition of the sulfur bond has a catalytic effect on the pyrolysis of the copolymer matrix. The situation for V_2O_5-mixed resin is totally different. The content of S in V_2O_5-mixed resin is a little bit lower than that in Co^{2+}-doped resin below 445 °C. But the formation of SO_4^{2-} causes the removal of sulfur structure in the resin, which facilitates the pyrolysis of copolymer matrix and the C content is significantly reduced at 445 °C. When the temperature is further increased to 515 °C and 630 °C, the content of S in the resin changes little, indicating that S is finally converted to stable SO_4^{2-} remaining in the solid residue. During this process, the residual copolymer matrix is further decomposed and the content of C eventually decreases almost to zero.

In summary, both doped Co^{2+} and V_2O_5 can promote the conversion and decomposition of the sulfur bond at low temperatures in the pyrolysis of resin, which further promotes the pyrolysis of the copolymer matrix. But their effects are different. For Co^{2+}-doped resin, the decomposition of -S- completes at 515 °C, and the copolymer matrix begins to be pyrolyzed dramatically, after which the -S- is mainly converted to SO_4^{2-}. The V_2O_5-mixed resin removes partial -SO_3H and forms SO_4^{2-} at 445 °C, so that the copolymer matrix begins to be pyrolyzed at the same time. The remaining -SO_3H transforms into -S-, which is converted to SO_4^{2-} at 630 °C. It is understandable that the doped Co^{2+} is uniformly distributed in the resin with high contact efficiency to the sulfur structure, resulting in the better catalytic effect on the conversion of -S-. But how does a physical blending of V_2O_5 with resin play a better catalytic role than other oxides? And how could V_2O_5 directly remove partial -SO_3H at a lower temperature and promote the pyrolysis of the copolymer matrix at such temperatures and finally reduce the residue of resin? To answer those questions the catalytic mechanism of V_2O_5 was further studied and is described in the following part.

3.3 Catalytic mechanism of V_2O_5

According to the literature on the mechanism of metal oxide catalysts, oxides such as CuO and CoO have higher adsorption capacity for gas-phase oxygen because of their large number of oxygen vacancies (Juang and Lee, 2002). The adsorbed O_2 is activated to form active oxygen species (O_2^-, O^-, and O^{2-}) (Freund et al., 1996; Triguero et al., 1999; Juang and Lee, 2002; Wang and Barteau, 2003), which promote the decomposition of -S- and decrease the pyrolysis temperature of the copolymer matrix. The catalytic effect of doped Co^{2+} is also due to the formation of its oxides with good dispersibility in the oxidative pyrolysis process of resins. Therefore, the oxidation-reduction performance and oxygen storage performance of various metal oxides were investigated by H_2-TPR and O_2-TPD in order to study the catalytic effect of V_2O_5.

The oxidation-reduction performance of each metal oxide was analyzed by H_2-TPR, and the results are shown in Fig. 5. The hydrogen consumptions of different catalysts from TPR are presented in Table 2. The peak in the H_2-TPR spectrum represents a reducible species, and the peak temperature corresponds to the degree of difficulty of the reduction of the oxide, and the peak area is proportional to the amount of the oxide species. As shown in Fig. 5, the reduction peaks of CuO, Co_2O_3, Co_3O_4, and CoO are all located at 300–500 °C, which is significantly lower than the reduction peak of V_2O_5 at 650–700 °C. This indicates that CuO, Co_2O_3, Co_3O_4, and CoO are more easily reduced by H_2 than V_2O_5 is. In addition, the hydrogen consumptions of CuO, Co_2O_3, Co_3O_4, and CoO are all higher than 0.320 mmol/g, which is larger than the 0.260 mmol/g of V_2O_5. So the ease of reduction by the different catalysts is CoO>CuO>Co_2O_3≈Co_3O_4>V_2O_5.

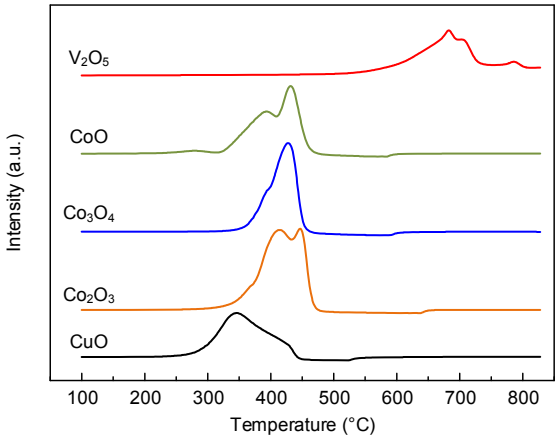

Fig. 5 H_2-TPR curves of different catalysts

Table 2 H_2 consumption, O_2 desorption, CO_2 desorption, and NH_3 desorption amounts of different catalysts from TPR/TPD

Catalyst	H_2 consumption (mmol/g)	O_2 desorption (mmol/g)	CO_2 desorption (mmol/g)	NH_3 desorption (mmol/g)
V_2O_5	0.260	0.011	0.027	0.126
CoO	0.386	0.030	0.027	0.088
Co_3O_4	0.320	0.018	0.016	0.062
Co_2O_3	0.323	0.002	0.011	0.031
CuO	0.363	0.002	0.001	0.002

The oxygen storage performance (lattice oxygen and adsorbed oxygen) of each metal oxide was examined by O_2-TPD, and the results are shown in Fig. 6. The oxygen desorption amounts of different catalysts from TPD are presented in Table 2. The peaks in the O_2-TPD spectrum represent the oxygen species. The desorption of lattice oxygen requires a certain amount of energy, so the desorption peaks are generally above 500 °C. The adsorption peaks (physical and chemical adsorption) are often below 500 °C (Royer et al., 2005; Zhu et al., 2005; Sutthiumporn and Kawi, 2011). It can be seen from Fig. 6 that the O_2 desorption peaks appear at 530–800 °C, corresponding to the desorption peaks of the lattice oxygen. At the same time, this temperature range is close to the pyrolysis temperature of the resin copolymer matrix, which also indicates that the catalytic effect of metal oxides may be related to the reactive oxygen species produced (Sutthiumporn and Kawi, 2011). Fig. 6 and Table 2 also explain why doped Co^{2+} has a better catalytic effect than V_2O_5. On the one hand, the desorption peak temperature of CoO is lower than V_2O_5 but, on the other hand, the oxygen desorption amount of V_2O_5 is 0.011 mmol/g, which is smaller than the 0.030 mmol/g of CoO, indicating that the amount of lattice oxygen in V_2O_5 is less than that of CoO. The oxygen desorption amounts of the different catalysts are in the order $CoO>Co_3O_4>V_2O_5>Co_2O_3\approx CuO$. The results show that the oxygen storage performance of V_2O_5 is not the greatest among these five metal oxides and is significantly weaker than that of CoO.

According to the results of H_2-TPR and O_2-TPD, the ease of reduction by V_2O_5 is lower than that of CuO, Co_2O, Co_3O_4, and CoO, and its oxygen storage performance is not outstanding. This result is consistent with the experimental results in Section 3.2. Combined with previous studies (Matsuda et al., 1986b; Juang and Lee, 2002), the catalytic mechanism of doped Co^{2+} for oxidative pyrolysis of resin is that the active oxygen species, which is produced by the formed cobalt oxides after adsorption of oxygen, promotes the oxidative pyrolysis of the copolymer matrix. So the structure is pyrolyzed at a lower temperature. As the ease of reduction of V_2O_5 is lower than that of Co_2O_3, Co_3O_4, and CoO, and its oxygen storage performance is unremarkable, the catalytic effect on temperature decrease of V_2O_5 is weaker than that of doped Co^{2+}. However, from the view of active oxygen species, it is difficult to explain why the physically blended V_2O_5 not only has a catalytic effect on temperature decrease but also can reduce the amount of residue.

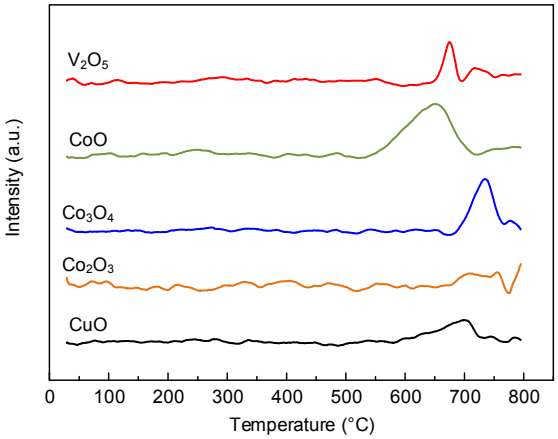

Fig. 6 O_2-TPD curves of different catalysts

Considering the metal oxides as catalysts, in addition to the catalytic effect resulting from oxidisation, it may also arise from acidity and alkalinity (Haber et al., 1997). Therefore, the alkali sites of each oxide were analyzed by CO_2-TPD at first, and the results are shown in Fig. 7. The CO_2 desorption amounts of different catalysts from TPD are presented in Table 2. The peaks in the CO_2-TPD spectrum represent the alkali sites. In general, the CO_2 desorption peaks of the five catalysts are not obvious, and the amounts of the alkali sites are also low and are all less than 0.030 mmol/g. The relative strength order of alkali sites is $V_2O_5\approx CoO>Co_3O_4>Co_2O_3>CuO$. Although the alkali sites of V_2O_5 are stronger than those

of Co_3O_4, Co_2O_3, and CuO, that is not the reason why V_2O_5 has a better catalytic performance. As the alkalinity of CoO is not much different from that of V_2O_5, but the catalytic performance of CoO is poor, it is indicated that their different catalytic performances are not due to alkalinity.

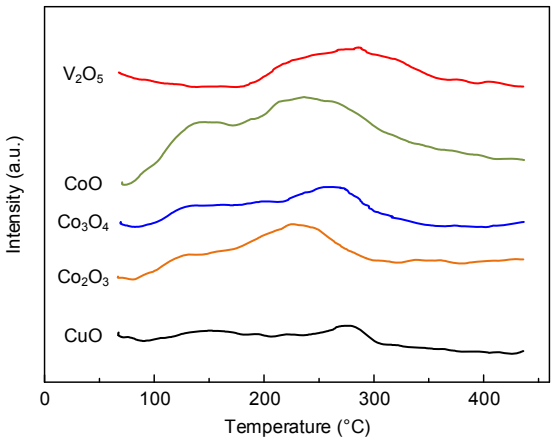

Fig. 7 CO_2-TPD curves of different catalysts

Finally, the acid sites of each oxide were investigated by NH_3-TPD, and the results are shown in Fig. 8. The NH_3 desorption amounts of different catalysts from TPD are presented in Table 2. The peak in the NH_3-TPD spectrum represents the temperature at which NH_3 can be desorbed. The higher the desorption peak temperature, the more difficult it is for the catalyst to desorb NH_3, indicating that the acid site is stronger. The five metal oxides all have a broad NH_3 desorption peak at 100–300 °C, which belongs both to the weak acid site and the medium-strong acid site (Turco et al., 2007). In Table 2, the amount of V_2O_5 acid sites, which is 0.126 mmol/g, is obviously larger than those of the other four catalysts, and the relative strength order of acid sites is: V_2O_5>CoO>Co_3O_4>Co_2O_3>CuO. This is exactly the difference between V_2O_5 and other catalysts. But how does V_2O_5 produce its catalytic effect by its acidity? On the one hand, combining data in the literature (Sviridova et al., 2013; Tomskii et al., 2017) and the results of NH_3-TPD, the acid sites showing a catalytic effect in this study mainly refer to the weak Lewis acid sites of 200–300 °C in the curves. The Lewis acid sites are capable of adsorbing and activating polarized hydrocarbon molecules and thiol molecules (Corma and Orchillés, 2000; Hernández-Beltrán et al., 2004). In the pyrolysis process of the resin, the sulfonic acid groups transform into sulfur bonds, which will cross-link with the copolymer matrix to form thioether. The sulfur bond in the thioether has two lone pair electrons, which can attract the Lewis acid sites on V_2O_5. The process can be represented in formula (1):

$$V^{n+}\text{-O-V} + \text{R-}\ddot{\text{S}}\text{-R} \longrightarrow \begin{matrix}\text{V-O-V}\\ \vdots\\ \text{R-S-R}\end{matrix} \quad (1)$$

Therefore, although V_2O_5 is mixed with resin by physical blending, it can directly adsorb to the sulfur bond through the acid sites to play an oxidative role. Moreover, even if the oxidability of V_2O_5 is weaker than that of CoO and CuO, V_2O_5 can still exert a good catalytic effect to promote the oxidative pyrolysis of resin while CoO and CuO cannot do so. However, compared with the doped Co^{2+} which is directly bonded to the sulfonic acid groups, since the oxidizing effect of V_2O_5 is weaker than that of CoO, the decrease of final pyrolysis temperature is smaller. On the other hand, results in the literature (Jason, 1993; Patterson et al., 2001; Nambo et al., 2016) indicate that the removal of sulfonic acid groups in aromatic sulfonic acids usually requires acid catalysis. So the acidity of V_2O_5 may also catalyze the removal of sulfonic acid groups at low temperature (445 °C) to some extent. The removal of -SO_3H further promotes the decomposition of the copolymer matrix at lower temperatures and reduces the pyrolysis residue.

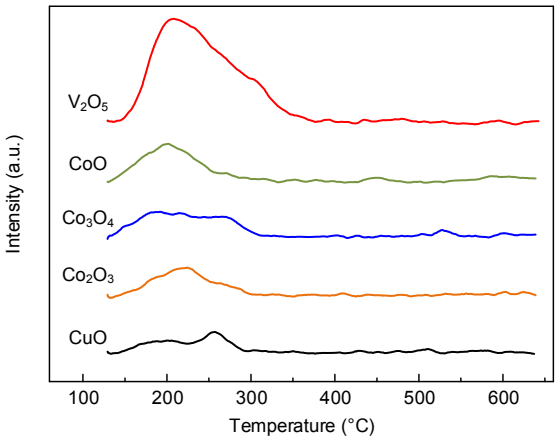

Fig. 8 NH_3-TPD curves of different catalysts

In summary, in order to simultaneously achieve the dual purpose of decreasing the temperature and

reducing the residue, the catalyst for pyrolysis of cation exchange resin needs both oxidation-reduction centers and acid sites. Those acid sites may have a greater influence on the oxidative pyrolysis reaction of the resin because of its absorbability by the sulfur structure. The catalytic mechanism of V_2O_5 on resin pyrolysis can be expressed as shown in Fig. 9, and it can be divided into two parts. The first part is that V_2O_5 may be helpful in removing a small part of accessible sulfonic acid groups directly at a lower temperature (445 °C) to form sulfates (SO_4^{2-}), and promote the pyrolysis of the copolymer matrix into hydrocarbons (C_xH_y) to reduce the residue. That mechanism is proposed based on the experimental phenomena shown in Figs. 3 and 4. When the temperature is higher than 445 °C, most of the sulfonic acid groups will transform into the sulfur bond (-S-), which will cross-link with the copolymer matrix to form thioether. The sulfur bond in the thioether structure has two lone pair electrons. The second part of the catalytic mechanism is then that V_2O_5, with a large number of Lewis acid sites, can be in close contact with the sulfur bond by chemisorption and can then exert the catalytic effect of the oxidation-reduction centers through physical blending. Finally, the sulfur bond structure is destroyed under the redox, and the copolymer matrix is pyrolyzed subsequently at 445–630 °C. Therefore, V_2O_5 displays a better catalytic effect on the pyrolysis of the resin than CuO, Co_2O_3, Co_3O_4, or CoO.

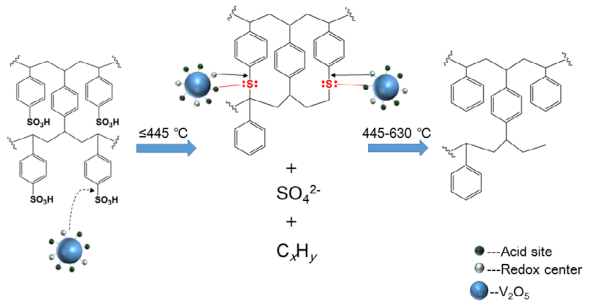

Fig. 9 Catalytic mechanism of V_2O_5
Dotted line indicates a suggested mechanism based on experimental phenomena

4 Conclusions

In this study, V_2O_5 is mixed with cation exchange resin by physical blending, and shows good catalytic effects on the oxidative pyrolysis of the resin. Compared to the oxidative pyrolysis of pure resin, when the mass ratio of V_2O_5 to resin is increased from 0.05 to 0.20, the peak temperature of the weight loss peak of the copolymer matrix is lowered by 140 °C to 173 °C, and the mass fraction of the pyrolysis product is decreased by 5% to 11.9%. Compared with other common catalysts (CuO, Co_2O_3, Co_3O_4, CoO, and doped Co^{2+}), this is the best catalyst and shows good catalytic performance by physical blending achieving the decrease of final pyrolysis temperature and of residue simultaneously.

Further analysis shows that V_2O_5 and doped Co^{2+} can both promote the conversion and decomposition of the sulfur bond, which will facilitate the pyrolysis of the copolymer matrix significantly at lower temperatures compared with pure resin. In addition, V_2O_5 can remove partial sulfonic acid groups to form SO_4^{2-} at 445 °C, resulting in the pyrolysis of the copolymer matrix, which decreases the residue of the resin.

By investigating the oxidation-reduction performance, oxygen storage performance, and the alkali and acid sites of different catalysts, it is found that although the oxidizing power of V_2O_5 is relatively weak, its number of acid sites is the highest. Its catalytic effect is achieved by its acid sites and its oxidation-reduction centers. Under the effect of the acid sites, V_2O_5 can be in close contact with the sulfur bond through chemisorption to further exert the catalytic effect of oxidation-reduction centers, although it is added by physical blending. Moreover, V_2O_5 may also promote desulfonation at lower temperatures and further decrease the residue.

Contributors

Yao YANG designed the research. Qi SONG, Jian-hua SHEN, and Yong YANG performed the tests and processed the corresponding data. Qi SONG wrote the first draft of the manuscript. Yao YANG, Bin-bo JIANG, and Zu-wei LIAO helped to organize the manuscript and revised and edited the final version.

Conflict of interest

Qi SONG, Jian-hua SHEN, Yong YANG, Yao YANG, Bin-bo JIANG, and Zu-wei LIAO declare that they have no conflict of interest.

References

Chun UK, Choi K, Yang KH, et al., 1998. Waste minimization

pretreatment via pyrolysis and oxidative pyroylsis of organic ion exchange resin. *Waste Management*, 18(3): 183-196.
https://doi.org/10.1016/s0956-053x(98)00020-8

Corma A, Orchillés AV, 2000. Current views on the mechanism of catalytic cracking. *Microporous and Mesoporous Materials*, 35-36:21-30.
https://doi.org/10.1016/s1387-1811(99)00205-x

Eun HC, Yang HC, Cho YZ, et al., 2009. Study on a stable destruction method of radioactive waste ion exchange resins. *Journal of Radioanalytical and Nuclear Chemistry*, 281(3):585-590.
https://doi.org/10.1007/s10967-009-0034-6

Freund HJ, Kuhlenbeck H, Staemmler V, 1996. Oxide surfaces. *Reports on Progress in Physics*, 59(3):283-347.
https://doi.org/10.1088/0034-4885/59/3/001

Haber J, Witko M, Tokarz R, 1997. Vanadium pentoxide I. Structures and properties. *Applied Catalysis A: General*, 157(1-2):3-22.
https://doi.org/10.1016/s0926-860x(97)00017-3

Hamodi N, Papadopoulou K, Lowe T, et al., 2012. Thermal analysis and immobilisation of spent ion exchange resin in borosilicate glass. *New Journal of Glass and Ceramics*, 2(3):111-120.
https://doi.org/10.4236/njgc.2012.23016

Hernández-Beltrán F, Quintana-Solórzano R, Sánchez-Valente J, et al., 2004. On the effect of a high reactive sulfur species on sulfur reduction in gasoline. *Studies in Surface Science and Catalysis*, 149:355-367.
https://doi.org/10.1016/S0167-2991(04)80774-2

Hou JL, Ma Y, Li SY, et al., 2018. Transformation of sulfur and nitrogen during Shenmu coal pyrolysis. *Fuel*, 231:134-144.
https://doi.org/10.1016/j.fuel.2018.05.046

Hu HY, Fang Y, Liu H, et al., 2014. The fate of sulfur during rapid pyrolysis of scrap tires. *Chemosphere*, 97:102-107.
https://doi.org/10.1016/j.chemosphere.2013.10.037

Jantzen CM, 2006. Characterization and performance of fluidized bed steam reforming (FBSR) product as a final waste form. *In*: Vienna JD, Spearing DR (Eds.), Environmental Issues and Waste Management Technologies in the Ceramic and Nuclear Industries IX. American Ceramic Society, Westerville, USA, p.319-329.
https://doi.org/10.1002/9781118407004.ch30

Jantzen CM, Lorier TH, Pareizs JM, et al., 2007. Fluidized bed steam reformed (FBSR) mineral waste forms: characterization and durability testing. *In*: Dunn D, Poinssot C, Begg B (Eds.), Scientific Basis for Nuclear Waste Management XXX. Materials Research Society, Warrendale, USA, p.379-388.

Jantzen CM, Lee WE, Ojovan MI, 2013. Radioactive waste (RAW) conditioning, immobilization, and encapsulation processes and technologies: overview and advances. *In*: Lee WE, Ojovan MI, Jantzen CM (Eds.), Radioactive Waste Management and Contaminated Site Clean-up: Processes, Technologies and International Experience. Woodhead Publishing, Philadelphia, USA, p.171-272.
https://doi.org/10.1533/9780857097446.1.171

Jason ME, 1993. The desulfonation of phenolsulfonic acids in aqueous sodium hydrogen sulfate mixtures. *Phosphorus, Sulfur, and Silicon and the Related Elements*, 79(1-4): 55-64.
https://doi.org/10.1080/10426509308034397

Juang RS, Lee TS, 2002. Oxidative pyrolysis of organic ion exchange resins in the presence of metal oxide catalysts. *Journal of Hazardous Materials*, 92(3):301-314.
https://doi.org/10.1016/s0304-3894(02)00025-0

Kim K, Son SH, Kim K, et al., 2010. Treatment of radioactive ionic exchange resins by super- and sub-critical water oxidation (SCWO). *Nuclear Engineering and Design*, 240(10):3654-3659.
https://doi.org/10.1016/j.nucengdes.2010.06.018

Mason JB, Myers CA, 2010. Thor® steam reforming technology for the treatment of ion exchange resins and more complex wastes such as fuel reprocessing wastes. Proceedings of ASME 13th International Conference on Environmental Remediation and Radioactive Waste Management, p.171-178.
https://doi.org/10.1115/ICEM2010-40165

Matsuda M, Funabashi K, Yusa H, 1986a. Effect of metallic impurities on oxidation reaction of ion exchange resin (I). Catalytic effect of ionized and unionized irons. *Journal of Nuclear Science and Technology*, 23(3):244-252.
https://doi.org/10.1080/18811248.1986.9734977

Matsuda M, Funabashi K, Yusa H, 1986b. Effect of metallic impurities on oxidation reaction of ion exchange resin (II). Comparison of catalytic activity between six metals. *Journal of Nuclear Science and Technology*, 23(9): 813-818.
https://doi.org/10.1080/18811248.1986.9735058

Matsuda M, Funabashi K, Yusa H, et al., 1987. Influence of functional sulfonic acid group on pyrolysis characteristics for cation exchange resin. *Journal of Nuclear Science and Technology*, 24(2):124-128.
https://doi.org/10.1080/18811248.1987.9735785

Moustakas K, Fatta D, Malamis S, et al., 2005. Demonstration plasma gasification/vitrification system for effective hazardous waste treatment. *Journal of Hazardous Materials*, 123(1-3):120-126.
https://doi.org/10.1016/j.jhazmat.2005.03.038

Myrstad T, Seljestokken B, Engan H, et al., 2000. Effect of nickel and vanadium on sulphur reduction of FCC naphtha. *Applied Catalysis A: General*, 192(2):299-305.
https://doi.org/10.1016/s0926-860x(99)00405-6

Nambo M, Ariki ZT, Canseco-Gonzalez D, et al., 2016. Arylative desulfonation of diarylmethyl phenyl sulfone with arenes catalyzed by scandium triflate. *Organic Letters*, 18(10):2339-2342.

https://doi.org/10.1021/acs.orglett.6b00744

Nezu A, Morishima T, Watanabe T, 2003. Thermal plasma treatment of waste ion-exchange resins doped with metals. *Thin Solid Films*, 435(1-2):335-339. https://doi.org/10.1016/s0040-6090(03)00364-x

Patterson DA, Metcalfe IS, Xiong F, et al., 2001. Wet air oxidation of linear alkylbenzene sulfonate 2. Effect of pH. *Industrial & Engineering Chemistry Research*, 40(23): 5517-5525. https://doi.org/10.1021/ie010294c

Pierce EM, Lukens WW, Fitts JP, et al., 2014. Experimental determination of the speciation, partitioning, and release of perrhenate as a chemical surrogate for pertechnetate from a sodalite-bearing multiphase ceramic waste form. *Applied Geochemistry*, 42:47-59. https://doi.org/10.1016/j.apgeochem.2013.12.017

Royer S, Bérubé F, Kaliaguine S, 2005. Effect of the synthesis conditions on the redox and catalytic properties in oxidation reactions of $LaCo_{1-x}Fe_xO_3$. *Applied Catalysis A: General*, 282(1-2):273-284. https://doi.org/10.1016/j.apcata.2004.12.018

Shen JH, Song Q, Yao B, et al., 2019. Catalytic effect of cobalt ion on oxidative pyrolysis of cation exchange resin. *CIESC Journal*, 70(7):2548-2555 (in Chinese). https://doi.org/10.11949/0438-1157.20190253

Singare PU, Lokhande RS, Madyal RS, 2011. Thermal degradation studies of some strongly acidic cation exchange resins. *Open Journal of Physical Chemistry*, 1(2):45-54. https://doi.org/10.4236/ojpc.2011.12007

Song Q, Shen JH, Yang Y, et al., 2020. Effect of temperature on the synthesis of sodalite by crystal transition process. *Microporous and Mesoporous Materials*, 292:109755. https://doi.org/10.1016/j.micromeso.2019.109755

Sutthiumporn K, Kawi S, 2011. Promotional effect of alkaline earth over Ni-La_2O_3 catalyst for CO_2 reforming of CH_4: role of surface oxygen species on H_2 production and carbon suppression. *International Journal of Hydrogen Energy*, 36(22):14435-14446. https://doi.org/10.1016/j.ijhydene.2011.08.022

Sviridova TV, Antonova AA, Boikov EV, et al., 2013. Oxidation of benzene and thiophene on a nanostructured vanadium-molybdenum mixed oxide. *Russian Journal of Physical Chemistry B*, 7(2):118-122. https://doi.org/10.1134/S1990793113020140

Tang H, Xu M, Hu HY, et al., 2018. In-situ removal of sulfur from high sulfur solid waste during molten salt pyrolysis. *Fuel*, 231:489-494. https://doi.org/10.1016/j.fuel.2018.05.123

Tomskii IS, Vishnetskaya MV, Vakhrushin PA, et al., 2017. Oxidative desulfurization of straight-run diesel fraction on vanadium–molybdenum catalysts. *Petroleum Chemistry*, 57(10):908-913. https://doi.org/10.1134/S0965544117100188

Triguero L, de Carolis S, Baudin M, et al., 1999. Metal oxides: O^{2-} chemistry and dynamical effects on oxide reactivity. *Faraday Discussions*, 114:351-362. https://doi.org/10.1039/a904987h

Turco M, Bagnasco G, Cammarano C, et al., 2007. Cu/ZnO/Al_2O_3 catalysts for oxidative steam reforming of methanol: the role of Cu and the dispersing oxide matrix. *Applied Catalysis B: Environmental*, 77(1-2):46-57. https://doi.org/10.1016/j.apcatb.2007.07.006

Wan Z, Xu LJ, Wang JL, 2016. Treatment of spent radioactive anionic exchange resins using fenton-like oxidation process. *Chemical Engineering Journal*, 284:733-740. https://doi.org/10.1016/j.cej.2015.09.004

Wang DX, Barteau MA, 2003. Differentiation of active oxygen species for butane oxidation on vanadyl pyrophosphate. *Catalysis Letters*, 90(1-2):7-11. https://doi.org/10.1023/a:1025836831303

Wang JL, Wan Z, 2015. Treatment and disposal of spent radioactive ion-exchange resins produced in the nuclear industry. *Progress in Nuclear Energy*, 78:47-55. https://doi.org/10.1016/j.pnucene.2014.08.003

Yang HC, Lee MW, Yoon IH, et al., 2013. Scale-up and optimization of a two-stage molten salt oxidation reactor system for the treatment of cation exchange resins. *Chemical Engineering Research and Design*, 91(4): 703-712. https://doi.org/10.1016/j.cherd.2013.02.014

Zahorodna M, Bogoczek R, Oliveros E, et al., 2007. Application of the Fenton process to the dissolution and mineralization of ion exchange resins. *Catalysis Today*, 129(1-2): 200-206. https://doi.org/10.1016/j.cattod.2007.08.014

Zhang LD, Li YH, 2015. Investigation on treatment technology of radioactive spent resin and discussion on route selection. *Science Times*, (14):73-74 (in Chinese).

Zhu JJ, Zhao Z, Xiao DH, et al., 2005. Study of $La_{2-x}Sr_xCuO_4$ (x=0.0, 0.5, 1.0) catalysts for NO+CO reaction from the measurements of O_2-TPD, H_2-TPR and cyclic voltammetry. *Journal of Molecular Catalysis A: Chemical*, 238(1-2):35-40. https://doi.org/10.1016/j.molcata.2005.03.036

List of electronic supplementary materials

Fig. S1 Thermogravimetric curves of catalysts